11,12 -Epoxyeicosatrienoic acid (11,12 EET) reduces excitability and excitatory transmission in the hippocampus

Mule, Nandkishor K ; Orjuela Leon, Anette C ; Falck, John R ; Arand, Michael ; Marowsky, Anne

Abstract: Recent studies suggest a role for the arachidonic acid-derived epoxyeicosatrienoic acids (EETs) in attenuating epileptic seizures. However, their effect on neurotransmission has never been investigated in detail. Here, we studied how 11,12- and 14,15 EET affect excitability and excitatory neurotransmission in mouse hippocampus. 11,12 EET (2 M), but not 14,15 EET (2 M), induced the opening of a hyperpolarizing K+ conductance in CA1 pyramidal cells. This action could be blocked by BaCl2, the G protein blocker GDP -S and the GIRK1/4 blocker tertiapin Q and the channel was thus identified as a GIRK channel. The 11,12 EET-mediated opening of this channel significantly reduced excitability of CA1 pyramidal cells, which could not be blocked by the functional antagonist EEZE (10 M). Furthermore, both 11,12 EET and 14,15 EET reduced glutamate release on CA1 pyramidal cells with 14,15 EET being the less potent regioisomer. In CA1 pyramidal cells, 11,12 EET reduced the amplitude of excitatory postsynaptic currents (EPSCs) by 20% and the slope of field excitatory postsynaptic potentials (fEPSPs) by 50%, presumably via a presynaptic mechanism. EEZE increased both EPSC amplitude and fEPSP slope by 40%, also via a presynaptic mechanism, but failed to block 11,12 EET-mediated reduction of EPSCs and fEPSPs. This strongly suggests the existence of distinct targets for 11,12 EET and EEZE in neurons. In summary, 11,12 EET substantially reduced excitation in CA1 pyramidal cells by inhibiting the release of glutamate and opening a GIRK channel. These findings might explain the therapeutic potential of EETs in reducing epileptiform activity.

DOI: https://doi.org/10.1016/j.neuropharm.2017.05.013

Neuropharmacology 123 (2017) 310–321

Contents lists available at ScienceDirect

Neuropharmacology

journal homepage: www.elsevier.com/locate/neuropharm

11,12 -Epoxyeicosatrienoic acid (11,12 EET) reduces excitability and excitatory transmission in the hippocampus

Nandkishor K. Mule [a], Anette C. Orjuela Leon [a], John R. Falck [b], Michael Arand [a], Anne Marowsky [a, *]

[a] Institute of Pharmacology and Toxicology, University of Zurich, Winterthurerstr. 190, 8057 Zurich, Switzerland
[b] Department of Biochemistry, Southwestern Medical Center, Dallas, Tx, USA

ARTICLE INFO

Article history:
Received 30 January 2017
Received in revised form
25 April 2017
Accepted 13 May 2017
Available online 17 May 2017

Keywords:
EETs
Soluble epoxide hydrolase
Neurotransmission
Hippocampus
GIRK channel
Epilepsy

ABSTRACT

Recent studies suggest a role for the arachidonic acid-derived epoxyeicosatrienoic acids (EETs) in attenuating epileptic seizures. However, their effect on neurotransmission has never been investigated in detail. Here, we studied how 11,12- and 14,15 EET affect excitability and excitatory neurotransmission in mouse hippocampus. 11,12 EET (2 μM), but not 14,15 EET (2 μM), induced the opening of a hyperpolarizing K^+ conductance in CA1 pyramidal cells. This action could be blocked by $BaCl_2$, the G protein blocker GDPβ-S and the GIRK1/4 blocker tertiapin Q and the channel was thus identified as a GIRK channel. The 11,12 EET-mediated opening of this channel significantly reduced excitability of CA1 pyramidal cells, which could not be blocked by the functional antagonist EEZE (10 μM). Furthermore, both 11,12 EET and 14,15 EET reduced glutamate release on CA1 pyramidal cells with 14,15 EET being the less potent regioisomer. In CA1 pyramidal cells, 11,12 EET reduced the amplitude of excitatory postsynaptic currents (EPSCs) by 20% and the slope of field excitatory postsynaptic potentials (fEPSPs) by 50%, presumably via a presynaptic mechanism. EEZE increased both EPSC amplitude and fEPSP slope by 40%, also via a presynaptic mechanism, but failed to block 11,12 EET-mediated reduction of EPSCs and fEPSPs. This strongly suggests the existence of distinct targets for 11,12 EET and EEZE in neurons. In summary, 11,12 EET substantially reduced excitation in CA1 pyramidal cells by inhibiting the release of glutamate and opening a GIRK channel. These findings might explain the therapeutic potential of EETs in reducing epileptiform activity.

1. Introduction

Lipid signaling molecules in the central nervous system (CNS) are diverse, including prominent eicosanoids such as the arachidonic acid (AA) derivatives endocannabinoids and prostaglandins. Lesser known are the AA-derived epoxyeicosatrienoic acids (EETs), which are synthesized by cytochrome P450 (CYP) epoxygenases. Due to the four double bonds in AA, four EET regioisomers are formed: 5,6-, 8,9-, 11,12- and 14,15-EET, with each regioisomer consisting of a mixture of R/S and S/R enantiomers (Capdevila et al., 2000). Although often considered as a single entity, several studies suggest that EETs act in a regioisomer- and enantiomer-specific manner (Ding et al., 2014; Lu et al., 2002; Node et al., 2001; Wang et al., 2008; Zou et al., 1996).

Generally, the relative quantities of EET regioisomers vary with the CYP isoenzyme present in the respective tissue. Of the 160 CYP isoenzymes in the mouse, members of the CYP2C and CYP2J family are most commonly considered to exert the highest epoxygenase activity toward AA (Spector and Norris, 2007). However, it should be noted that several other CYP isoforms also act as epoxygenases and generate EETs such as rat CYP2D18 (Thompson et al., 2000) and mouse CYP4X1 (Al-Anizy et al., 2006). The CNS cell types expressing epoxygenases comprise endothelial cells, astrocytes and neurons (reviewed in (Iliff et al., 2010b)). Specifically, the epoxygenases CYP4X1 (Al-Anizy et al., 2006), CYP2C29, CYP2C38 (Luo et al., 1998), CYP2J9 (Qu et al., 2001), CYP2J8, CYP2J11, CYP2J13 (Graves et al., 2013) and CYP2J5 (Allen brain atlas (Lein et al., 2007), http://www.brainmap.org) were identified in mouse brain. EETs are released in a calcium- and activity-dependent manner from diverse CNS cells, including sensory neurons (Sisignano et al., 2012) and astrocytes (Alkayed et al., 1997). However, if they are exclusively

* Corresponding author.
E-mail address: marowsky@pharma.uzh.ch (A. Marowsky).

http://dx.doi.org/10.1016/j.neuropharm.2017.05.013

synthesized on demand like most AA metabolites or released from endogenous EET pools, in which they are present as esters of glycerophopsholipids (Capdevila et al., 2000), is still disputed.

Earlier studies established EETs as potent vasodilators with a central role in neurovascular coupling, the linking of neuronal activity via astrocytes to evoke cerebral arteriolar dilatory responses (Imig et al., 2011). Furthermore, EETs display angiogenic, anti-apoptotic and anti-inflammatory properties, which together with the vasodynamic effect probably underlie EET-mediated neuroprotection (Koerner et al., 2007; Li et al., 2012; Liu et al., 2016b). Further EET-mediated effects in the CNS include the release of neuropeptides (Iliff et al., 2010a) and powerful anti-nociception, which is observed after injection of 14,15 EET into the periaqueductal gray, the primary control center for descending pain modulation (Terashvili et al., 2008). The bioactivity of EETs is limited by their hydrolysis to, reportedly, less active diols (dihydroxyeicosatrienoic acids, DHETs), a reaction catalyzed predominantly by soluble epoxide hydrolase (sEH) in the mouse brain (Zhang et al., 2007). Consistent with this, inhibitors of sEH (sEHi) effectively increase EET levels *in vivo* and have garnered widespread attention for their potential therapeutic use in multiple disorders such as hypertension, stroke, dyslipidemia, pain, immunological and neurological diseases (Shen, 2010).

Still, the exact mechanisms by which EETs exert their various effects remain poorly defined. It is generally agreed that EETs may function as autocrine and paracrine effectors. Potential molecular targets include the K_{ATP} channel (Lu et al., 2002) and the calcium-activated BK channel (BK_{Ca}) (Campbell et al., 1996; Li and Campbell, 1997). More recently, EET-mediated modulation of TRP channels has received attention with several studies reporting effects of EETs on TRPV4 (Earley et al., 2005; Vriens et al., 2005; Watanabe et al., 2003), TRPC6 (Fleming et al., 2007), TRPA1 (Sisignano et al., 2012) and TRPV4-TRPC1 (Ma et al., 2015). However, EETs are less likely to bind to and activate an ion channel directly. They are rather thought to activate a G protein-coupled receptor (Carroll et al., 2006; Hayabuchi et al., 1998; Li and Campbell, 1997), which activates a signal transduction pathway that ultimately modulates ion channel functions.

Even though most of the channels modulated by EETs are widely expressed in the CNS, little is known about the effects of EETs on neuronal excitability and transmission. Three recent studies suggest a possible involvement of EETs in the attenuation of pharmacologically-induced epileptic seizures in mice: i) Seizures generated by inhibition of the GABAergic system, but not by inhibition of 4-AP sensitive K^+ channels, were attenuated by prior application of a sEHi (Inceoglu et al., 2013); ii) Diazepam in combination with a sEHi prevented progression of tetramethylenedisulfotetramine-induced tonic seizures and lethality in mice (Vito et al., 2014), and iii) sEHi treatment led to significant suppression of pilocarpine-induced seizures and an increase in the seizure-induction threshold of fully kindled mice compared to non-treated animals (Hung et al., 2015). However it should be noted that EETs are not the only sEH substrates in the brain; other substrates include epoxides from docosahexaenoic acid (DHA) and eicosapentaenoic acid (EPA), which exert at least partially similar effects to those observed with EETs (Morisseau et al., 2010). While these reports implied that EETs suppress rather than increase neuronal excitation, the only study examining EET-mediated effects on neurotransmission did not affirm this notion. Indeed, 14,15-EET and the sEHi AUDA were both shown to enhance excitatory synaptic transmission in mouse prefrontal cortex, presumably by promoting the insertion of glutamatergic receptors in the postsynaptic membrane (Wu et al., 2015).

In light of the recent evidence that EETs help to suppress epileptic seizures, we hypothesized that EETs are strong modulators of excitatory synaptic transmission and neuronal excitability in the hippocampus, a brain region central for memory and learning and often the starting point for temporal lobe epilepsy. Specifically, we wanted a) to identify potential pre- and/or postsynaptically located molecular targets, underlying the EET-mediated effect and b) to test, if the so-called functional EET antagonist 14,15-epoxyeicosa-5(Z)-enoic acid (EEZE) (Gauthier et al., 2002) is able to counteract EET-mediated actions on neuronal transmission and excitability.

In this study, we recorded from CA1 pyramidal cells (PCs) in mouse hippocampus, using the patch-clamp technique and field potential recordings, as well as the respective pharmacology to isolate excitatory events. Finally, to address the question how endogenous EETs affect epileptic seizures, the effect of the selective sEHi tAUCB was studied on epileptiform activity in the hippocampus.

2. Materials and methods

All experiments were performed in accordance with regulations of the University of Zurich and the veterinary department of the canton of Zurich, Switzerland, for animal handling and experimentation.

2.1. Immunohistochemistry

Distribution of CYP2J protein was visualized by immunoperoxidase staining of parasagittal sections from perfusion-fixed tissue of male 10 week-old C57Bl/6 mice. Mice were deeply anesthetized with Nembutal and perfused with 4% paraformaldehyde in 0.15 M phosphate buffer (pH 7.4). Brains were post-fixed for 3 h, cryoprotected with sucrose and sectioned with a microtome (40 μm). Sections were incubated overnight at 4 °C with the CYP2J antibody (rabbit, diluted 1:1000 (Qu et al., 2001) in Tris buffer, pH 7.4 containing 2% normal goat serum and 0.2% Triton-100. The next day, a biotinylated secondary antibody directed against rabbit (1:300 Jackson ImmunoResearch, West Grove, PA, USA) was applied for 30 min, followed by Vectastain elite kit processing (Vector Laboratories, Burlingame, CA, USA) and incubation with diaminobenzidine as chromogen. Sections were mounted onto gelatin-coated glass slides, air-dried, dehydrated, and coverslipped with Eukitt. Images were digitized with a high-resolution camera and processed using the software Mosaic (ExploraNova, La Rochelle, France).

2.2. Hippocampal slice preparation

C57Bl/6J mice were obtained from Charles River laboratories (Freiburg, Germany). Transverse hippocampal slices (350–400 μm thick) of male, 3–4 week old mice were obtained using a vibrating blade microtome, HM 650 V (Thermo Scientific, UK). Briefly, a mouse was anaesthetized and euthanized by decapitation. The brain was extracted and immediately transferred into ice-cold artificial cerebrospinal fluid (ACSF) equilibrated with 95% O_2 and 5% CO_2 containing (in mM) NaCl (125), $CaCl_2$ (2.5), $MgCl_2$ (1), $NaHCO_3$ (26), KCl (2.5), NaH_2PO_4 (1.25) and glucose (10). Slices were immediately transferred to an incubating chamber with ACSF at 35 °C for 20 min and thereafter kept at room temperature.

2.3. Electrophysiology

Slices were mounted on poly-L-lysine-coated coverslips and transferred to the recording chamber, where they were continuously superfused with ACSF at a rate of 1.8 ml/min. All experiments were performed at 30–32 °C using an in-line heating system.

Hippocampal formation and CA1 PCs were visualized by using an upright microscope (BX51Wl, Olympus), equipped with a 20x water-immersion objective, infrared/differential interference contrast (DIC) optics and an infrared video imaging camera (VX55, Till Photonics).

Patch pipettes with tip resistances of 3–5 MΩ were pulled from borosilicate glass (GC150F-10, Harvard apparatus, UK) with a horizontal puller (Zeitz instrument, Germany). For most experiments, pipettes were filled with a K-gluconate based internal solution containing (in mM): K-gluconate (145), EGTA (1), HEPES (10), MgATP (5), NaGTP (0.5) and NaCl (5). The pH was adjusted to 7.3 with KOH; osmolarity was 295–305 mOsm. For one set of experiments a CsCl-based internal solution was used containing (in mM): CsCl (100), $MgCl_2$ (2), EGTA (0.1), MgATP (2), NaGTP (0.3) and HEPES (40). The pH was adjusted to 7.3 with CsOH; osmolarity was 290–300 mOsm. For the recordings of evoked excitatory postsynaptic currents (EPSCs), CA1 PCs were held at a holding potential of $V_h = -70$ mV and a glass capillary filled with ACSF was placed in stratum radiatum on Schaffer collaterals (SCs). Stimuli were given at 0.1 Hz. Bicuculline (25 μM) was present throughout the entire experiment to block inhibitory transmission. To assess the paired pulse ratio, paired stimuli with interstimulus intervals of 50 ms were given. For miniature EPSCs (mEPSCs) recordings, tetrodotoxin (TTX, 1 μM) and bicuculline (25 μM) were added to the bath solution. Ramp recordings were carried out in presence of TTX (1 μM) with CA1 PCs initially voltage clamped at $V_h = -70$ mV and then ramped from −120 mV to −50 mV in 0.6 s. Before the start of a ramp experiment, cells were held in current clamp mode and current pulses of −10 pA were injected to determine the resting membrane potential (RMP), capacitance, and the input resistance R_{input} of the cell. EET-induced currents were normalized to cell capacitance and expressed as pA/pF. To monitor series resistance R_S and R_{input} throughout voltage-clamp recordings, a hyperpolarizing pulse of −5 mV (50 ms) was given at constant intervals. Recordings, in which R_S changed more than 20% were discarded. To assess the spiking ability of CA1 PCs, cells were held in current clamp and a rectangular current (0.8 s) was injected every minute with the amplitude adapted to the individual cell such that a robust number of action potentials was evoked. EET- and EEZE-induced changes in RMP and the numbers of action potentials were analyzed. Field excitatory postsynaptic recordings (fEPSPs) were recorded in 400 μm thick hippocampal slices with an ACSF-filled glass pipette used as recording pipette. fEPSPs were evoked by stimulating SCs at 0.1 Hz, using a wide-tip ACSF-filled glass capillary. Stimulation intensity, ranging from 20 to 150 μA, was adapted for each recording to obtain a sub-maximal fEPSP signal with minimal non-synaptic contamination. For the recording of population spikes and bicuculline-induced epileptic discharges, the stimulating electrode was again placed on SCs, the recording electrode on stratum pyramidale.

Data were recorded with a Multiclamp 700B amplifier (Axon instruments), filtered at 3–10 kHz and digitized at 20 kHz (A/D hardware from National instruments). Data were acquired and analyzed with IGOR Pro software (Wave Metrics, Lake Oswego). Spontaneous events were analyzed off-line with the Mini Analysis Program (Synaptosoft). Prism 5 (GraphPad, USA) was used for statistical analysis and preparation of the graphs. Appropriate statistical tests were employed as indicated. Results of several experiments are presented as average values ± standard error of mean (SEM).

2.4. Pharmacology

All drugs were bath applied except GDPβS, which was dissolved in the internal solution. Stock solutions of tAUCB (trans-4-(4-[3-adamantan-1-yl-ureido]-cyclohexyloxy)-benzoic acid; 10 mM; kindly provided by C. Morisseau) and bicuculline (Tocris) were prepared in DMSO. Stocks for Guanosine-5′-O (2-thiodiphosphate)(GDPßS)sodium salt (10 mM; Biolog, Germany), $BaCl_2$ (1 M; Sigma-Aldrich, Germany) and tetrodotoxin citrate (1 mM; ANAWA, Switzerland) were prepared in purified water (Millipore Systems, USA). EEZE, (±)11, 12- and (±)14, 15-EETs as well as 11,12-DHET were obtained from Cayman (Adipogen, Switzerland), dissolved in ethanol. They were dried under nitrogen gas and re-dissolved in ACSF (1–10 mM) before bath-application.

3. Results

3.1. CYP2J epoxygenase expression in mouse hippocampus

Detailed expression pattern for CYP epoxygenases in mouse hippocampus are rare. To our knowledge the only cellular distribution pattern so far available is the one for the isoenzyme CYP2J5, which is however based on mRNA expression (Allen brain atlas (Lein et al., 2007)). We studied the expression pattern of CYP2J proteins (as an example for a family of epoxygenases) by immunohistochemistry in brain slices from C57Bl/6J mice, using a CYP2J pan antibody (Qu et al., 2001). In the hippocampus, strong CYP2J immunoreactivity (IR) was detected in cell bodies of CA1-CA3 PCs as well as in their apical and basal dendritic fields with particularly strong IR detected in apical dendrites of CA1 PC in the stratum radiatum (See Fig. 1a).

3.2. Effects of tAUCB, 11,12-EET and EEZE on CA1 synaptic transmission

To ensure that exogenously applied EETs were not immediately eliminated by sEH, the dominant epoxide hydrolase in mouse hippocampus (Marowsky et al., 2009), the potent and selective sEHi tAUCB (Hwang et al., 2007) was used. In a first experiment, we tested if tAUCB alone exerted any effects on synaptic transmission. Stimulating SCs, we recorded EPSCs in CA1 PCs; tAUCB (1 μM) was bath-applied. EPSC amplitude, kinetic parameters (rise time and decay constants) as well as the holding current I_{hold} were not affected by tAUCB (Fig. 1b, Suppl.Table 1). All subsequent experiments in which EETs were applied were therefore carried out in presence of 1 μM tAUCB.

Of the four EET regioisomers, we chose the ones synthesized in highest quantities in the hippocampus, 11,12 and 14,15 EET (Sanchez-Mejia et al., 2008). The focus was on the 11,12-regioisomer, additional experiments were conducted with 14,15 EET for comparison. First, we evaluated the effect of 11,12 EET on EPSCs in CA1 PCs, voltage-clamped at $V_h = -70$ mV. EPSCs were evoked by two consecutive stimuli with an interstimulus interval of 50 ms in presence of bicuculline (25 μM) to block inhibitory transmission. Bath-application of 11,12 EET (2 μM) led to a rapid and significant reduction of both EPSC amplitudes with the first amplitude reduced to 78 ± 5% (n = 5, paired Student's *t* test, p = 0.0256*) and the second to 86 ± 4% (p = 0.0481*, Fig. 1c, c_1, e). Comparison of the paired pulse ratio (PPR: Amp2/Amp1) under control conditions and in presence of EETs revealed an increase from 1.94 ± 0.13 to 2.15 ± 0.1 (paired Student's *t* test, p = 0.032*). Such a change in paired-pulse facilitation is usually an indication for a presynaptic site of action. We next tested if the antagonist EEZE is able to block the EET-induced reduction of EPSCs. Application of EEZE (10 μM) significantly potentiated both EPSC amplitudes (Fig. 1d, d_1) to 141 ± 10% (Amp1, n = 9, paired Student's *t* test, p = 0.0026**) and 119 ± 8, respectively (Amp2, p = 0.043*). The concomitant change in the PPR from 2.13 ± 0.11 to 1.77 ± 0.10 (Fig. 1f; p = 0.00078***) again pointed to a presynaptic site of

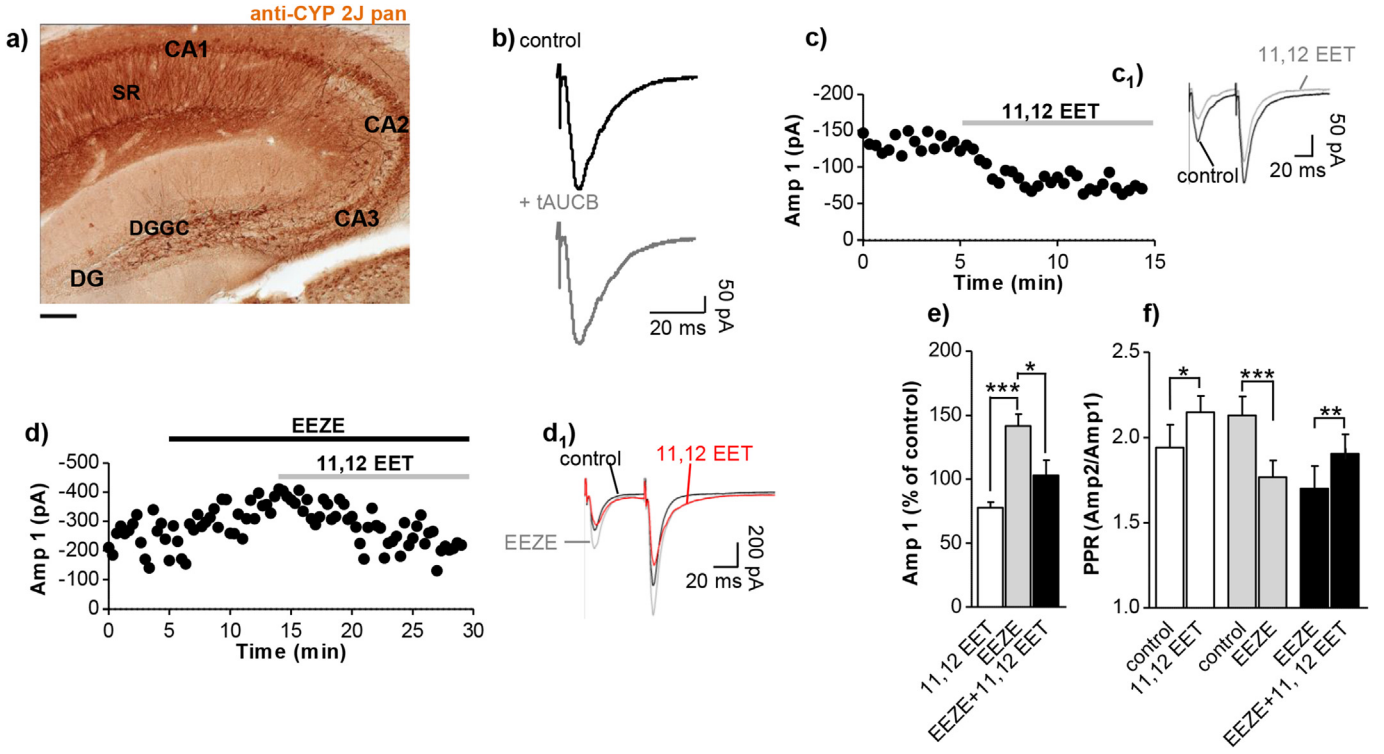

Fig. 1. 11,12 EET reduces, but EEZE potentiates EPSCs recorded in CA1 PCs.
a) CYP2J expression in mouse hippocampal formation illustrated by immunoperoxidase staining. Note the strong CYP2J IR in pyramidal cell bodies and particularly in CA1 dendrites, while dentate gyrus granule cells are spared. Scale bar: 250 μm; b) Representative traces of EPSCs before (upper graph) and after tAUCB (lower graph); summary of EPSC parameters are presented in Suppl. Table 1; c) Plot of EPSC peak amp 1 vs. time for a representative CA1 PC with the horizontal line indicating the time of bath-application of 2 μM 11,12 EET; c_1) Average of 10–20 traces from c) before and after application of 11,12 EET; d) Plot of EPSC peak amplitude vs. time for a representative CA1 PC exposed to the functional EET-antagonist EEZE (10 μM), followed by 11,12 EET (2 μM) as indicated by the horizontal lines; d_1) Average of 10–20 traces before and after application of EEZE and 11,12 EET; e) Summary of the effect of 11,12 EET (2 μM), EEZE (10 μM) and 11,12 EET (2 μM) +EEZE(10 μM) on EPSC amp; 1-way-ANOVA followed by Bonferroni, post-hoc analysis; for detailed data and statistics see Suppl. Table 2; f) Application of 11,12 EET, EEZE or 11,12 EET in presence of EEZE significantly changes the PPRs, suggesting presynaptic molecular targets for these compounds. $p < 0.05^{*}$, $p < 0.01^{**}$, $p < 0.001^{***}$. Abbreviations: CA cornu ammonis; DG dentate gyrus; DGGC dentate gyrus granule cells; SR stratum radiatum.

action. Surprisingly, prior application of EEZE followed by 11,12 EET was unable to prevent EET-mediated reduction of EPSC amplitudes (Fig. 1d). Moreover, even in the presence of EEZE, EETs still seemed to exert their effect by a presynaptic mechanism as indicated by the change in the PPR (Fig. 1f). (Detailed data for evoked EPSC recordings are shown in Suppl. Table 2).

To examine in more detail the presynaptic actions of EETs and EEZE, we next recorded mEPSCs in CA1 PCs in presence of TTX (1 μM) to abolish action potentials. mEPSCs are due to random release of single presynaptic glutamate vesicles at different synaptic sites. While application of 11,12 EET affected neither mEPSC amplitude nor frequency (n = 5, Fig. 2a-a_2, c), EEZE led to a rapid increase in the occurrence of mEPSCs, shown in Fig. 2b, b_1 and d (n = 5). However, EEZE had no consistent effect on mEPSC amplitudes in CA1 PCs (Fig. 2b_2, d). (Detailed data for mEPSCs recordings are shown in Suppl. Table 3). A change in mEPSC frequency is usually attributed to effects on quantal transmitter release and as such the effect is undisputedly of presynaptic origin. Taken together, the results indicate that EEZE affects transmitter release in the absence of action potentials, whereas 11,12 EET has no effect under these conditions. This strongly suggests two different presynaptic molecular targets.

In addition to the effect on EPSC amplitude, we observed another striking effect in some of the evoked EPSC and mEPSC experiments: The holding current I_{hold} was substantially modulated by 11,12 EET (see Figs. 2a and 3a), in a manner compatible with an increase in outward current. Re-analysis of the EET-mediated effect on I_{hold} in mEPSC recordings revealed that on average I_{hold} increased robustly by +21 ± 4 pA (n = 6, Student's paired *t* test p = 0.00615**, Fig. 3c, Suppl. Table 3). This increase in I_{hold} was accompanied by a decrease in input resistance (Fig. 3d), indicative of channel opening and the activation of a conductance. To gain further insight into the nature of the conductance, we repeated these experiments with a CsCl-based internal solution, as Cs^+ is known to block K^+ -conducting ion channels. Under these conditions, relative to the control, ΔI_{hold} and R_{input} were unchanged upon application of EETs (Fig. 3c,e). This demonstrates that no further conductance was activated and suggests that 11,12 EET activates a postsynaptic K^+ current.

3.3. Characterization of the 11,12 EET-induced current

For a more detailed characterization of the EET-activated current, we investigated its current-voltage relationship. To this end, current-voltage curves were obtained (n = 5) in the presence of TTX (1 μM). The 11,12 EET-induced current reversed at −102 ± 6 mV (Fig. 4a). These experiments were carried out with an extracellular K^+ concentration of 2.5 mM and an internal K^+ concentration of 145 mM (using a K-gluconate internal solution), therefore according to the Nernst equation the calculated K^+ reversal potential was −106 mV at 32 °C. The reversal potential determined by us was compatible with a K^+ current. For comparison, the same experiment was conducted with 14,15 EET (2 μM, n = 4); however, 14,15 EET failed to open any conductance in CA1 PCs (Fig. 4b). To narrow down the spectrum of possible K^+ channel candidates, we bath-applied 500 μM $BaCl_2$, a classical inhibitor of G protein-coupled

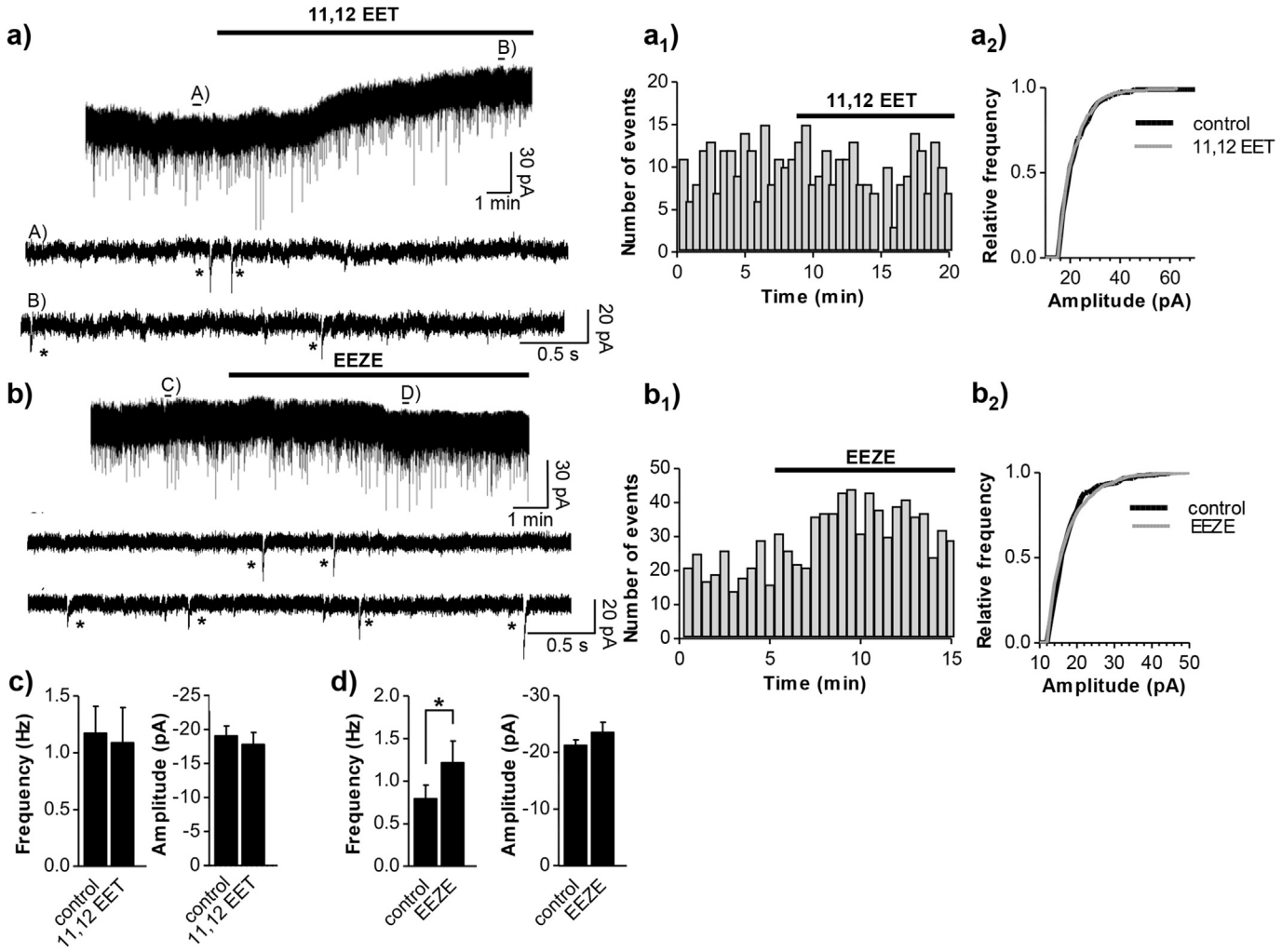

Fig. 2. EEZE modulates mEPSC frequency.
a) Representative trace of a mEPSC recording in a CA1 PC with application of 11,12 EET (2 μM) indicated by the horizontal line. Short horizontal lines marked with A) and B) denote stretches that are shown enlarged below to resolve the individual events, marked by asterisks; a_1) Frequency histogram for the mEPSC trace to the left; a_2) Cumulative probability plot depicting mEPSC amplitudes before and after addition of 11,12 EET for the mEPSC recording to the left. b) Representative trace of a mEPSC recording in a CA1 PC with application of EEZE (10 μM) indicated by the horizontal line. Horizontal lines marked with C) and D) denote short stretches shown enlarged below; b_1) Frequency histogram for the mEPSC trace to the left; b_2) Cumulative probability plot depicting mEPSC amplitudes before and after addition of EEZE for the mEPSC recording to the left; c) Summary of the 11,12 EET effect on mEPSC frequency and amplitude in CA1 PCs; d) Summary of the EEZE effect on mEPSC frequency and amplitude in CA1 PCs.

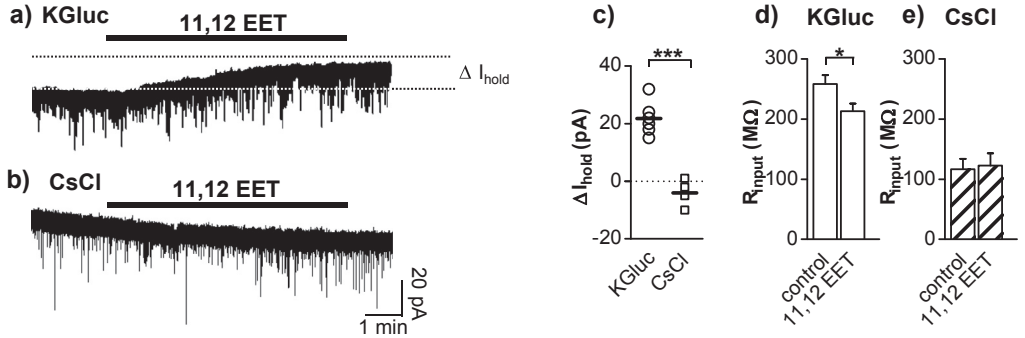

Fig. 3. 11,12 EET opens a postsynaptic Cs-sensitive conductance.
a) and b) representative traces of mEPSCs, $V_h = -70$ mV, recorded with a K-gluconate -based (a) and a CsCl-based (b) internal solution with 11,12 EET (2 μM) application indicated by horizontal lines. 11,12 EET potentiates the outward current only with the K-gluconate-based internal solution; c) and d) Summary of 11,12 EET-mediated changes in I_{hold} and R_{input}, recorded in CA1 PCs with the two different internal solution. $p < 0.05$*, $p < 0.001$***.

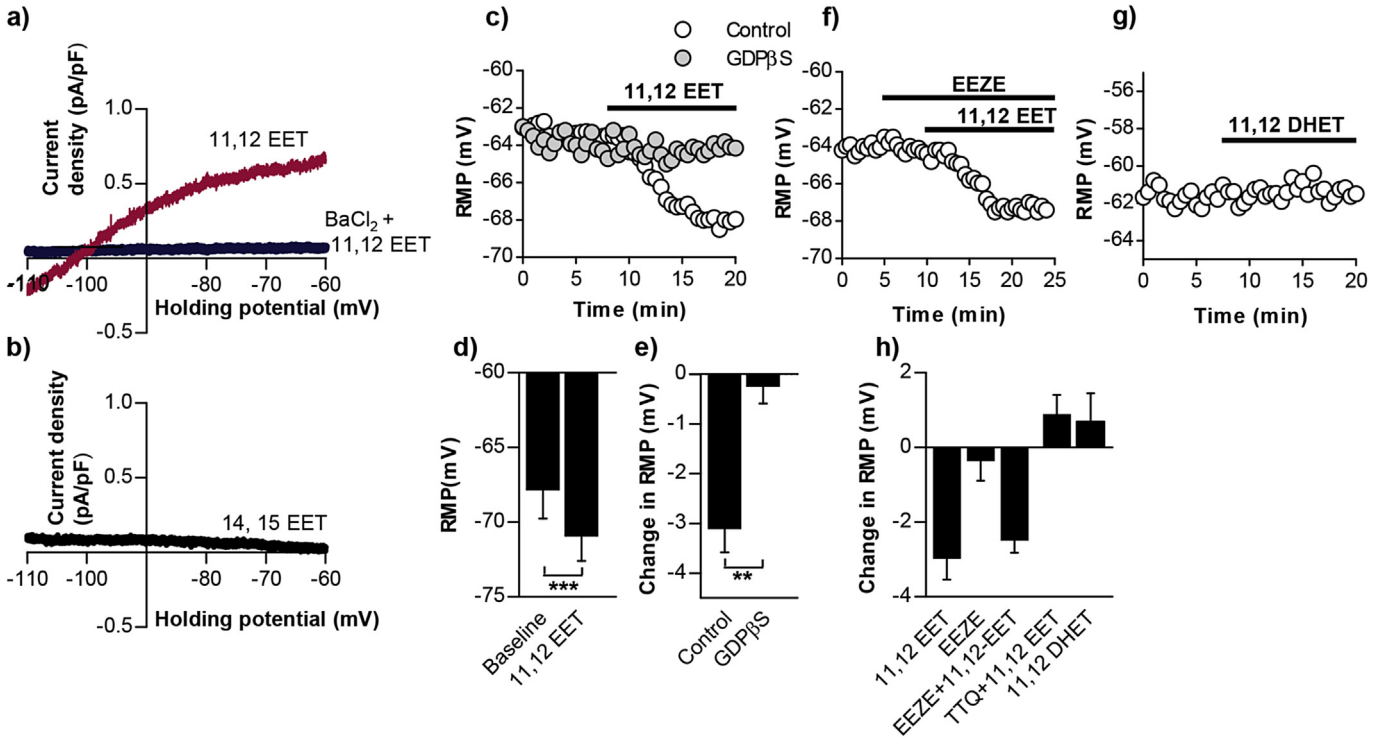

Fig. 4. 11,12 EET activates a GIRK1/4 conductance in CA1 PCs.
a)Voltage-clamp recordings of CA1 PCs with a K-gluconate-based internal solution. Red trace: A voltage ramp from −120 to −50 mV was applied in control condition and after bath application of 11,12 EET (2 μM). Control traces were subtracted from EET traces; the red trace represents the average of n = 5 cells. Blue trace: The same voltage ramp was applied in presence of 500 μM $BaCl_2$ followed by 11,12 EET (2 μM). $BaCl_2$ traces were subtracted from $BaCl_2$ + 11,12 EET traces. The blue trace represents the average of n = 8 cells. b) The same as a) with 14,15 EET (2 μM). The trace represents the average of n = 4 cells. Due to the lack of effect of 14,15 EET, no experiments were carried out in presence of $BaCl_2$; c) Example of current-clamp recordings of CA1 PCs to monitor RMP. The control cell (white circles) was dialyzed with normal K-gluconate based internal solution, while the other (gray circles) was dialyzed with the same internal solution containing 1 mM GDPβS. 11,12 EET (2 μM) was applied as indicated by the horizontal line; d) Average effect of 11,12 EET (2 μM) on RMP of control cells with normal internal solution; e) Comparison of 11,12 EETs-induced RMP change between control cells and those dialyzed with 1 mM GDPβS; f) Application of EEZE (10 μM) prior to 11,12 EET (2 μM) did not prevent EET-induced hyperpolarization in CA1 PCs, example trace of a representative cell; g) Application of 11,12 DHET had no effect on RMP, example trace of a representative cell; h) Summary graph of RMP changes after application of 11,12 EET (2 μM) or EEZE (10 μM) or 11,12 DHET (5 μM) alone, and in slices pretreated with EEZE (10 μM) or the selective GIRK1/4 blocker tertiapin Q (TTQ, 1 mM) followed by 11,12 EET (2 μM). (For interpretation of the references to colour in this figure legend, the reader is referred to the web version of this article.)

inward rectifier potassium (GIRK) channels (Sodickson and Bean, 1996), prior to 11,12 EET application (n = 8; Fig. 4a). In the presence of $BaCl_2$, 11,12 EET was unable to open a conductance. Since activation of GIRK channels modifies substantially the RMP of a neuron to more negative values, we next recorded CA1 PCs in current-clamp mode and monitored RMP before and after application of 11,12 EET; kynurenic acid and bicuculline were present throughout the experiment to suppress any spontaneous synaptic transmission. 11,12 EET hyperpolarized CA1 PC from −67.8 ± 1.8 mV to −70.9 ± 1.6 mV (Fig. 4d; n = 9, paired Student's *t* test p = 0.000217***) with an average of ΔRMP of −3.1 ± 0.5 mV (Fig. 4h).

EETs may open a GIRK channel either directly or via a G protein. To distinguish between these two scenarios, the G protein blocker GDPβS (1 mM) was included in the internal solution; to ensure complete diffusion, cells were dialyzed 20 min before the start of the recording (n = 5). GDPβS completely abolished EET-mediated hyperpolarization (Fig. 4c,e), verifying the involvement of a G-protein and refuting the notion of direct activation of a GIRK conductance by EETs. Final evidence for the EET-mediated activation of a GIRK current was obtained by bath-application of the selective GIRK1/4 (Kir3.1/3.4) blocker tertiapin Q (TTQ, 1 μM) prior to application of EETs. Under these conditions, 11,12 EET was unable to open an additional hyperpolarizing membrane conductance, and cells tended to depolarize slightly instead (n = 5, Fig. 4h).

EEZE alone had no effect on RMP and was unable to block EET-induced hyperpolarization in CA1 PCs, when washed in prior to 11,12 EET (Fig. 4f, h). Furthermore, the diol, 11,12 DHET (5 μM) was unable to induce a significant change in the RMP of CA1 PCs (Fig. 4g and h). Taken together, these results show that 11,12 EET opens, via a G protein-coupled mechanism, a GIRK 1/4 conductance in CA1 PCs, which leads to the observed hyperpolarization in these cells.

To assess if, and to what degree, the EET-activated GIRK current affects excitability of CA1 PCs, we studied the spiking ability of these cells in presence of 11,12 EET and EEZE. CA1 PCs were held in current-clamp mode and injected with a current pulse (Fig. 5a) to elicit a short train of action potentials. The injected current was adapted to the individual cell, ranging from +70 to +150 pA. Bath-application of 11,12 EET led to a hyperpolarization similar to that seen before (−3.4 ± 0.5, n = 9, data not shown) and reduced significantly the number of spikes to 76±%3 (n = 9, paired Student's *t* test p = 0.00012***; Fig. 5b). In presence of EEZE, the number of spikes was unchanged (n = 7, paired Student's *t* test, p = 0.175, Fig. 5c and d), and subsequent application of 11,12 EET reduced the number of spikes in a similar manner to that observed with 11,12 EET alone (75.0 ± 6%, paired Student's *t* test, p = 0.00018***; Fig. 5c and d).

3.4. Net effects of EETs and EEZE on hippocampal fEPSPs

Next, we addressed if as a net effect in the hippocampus EETs and EEZE dampen or increase excitatory neurotransmission. To this

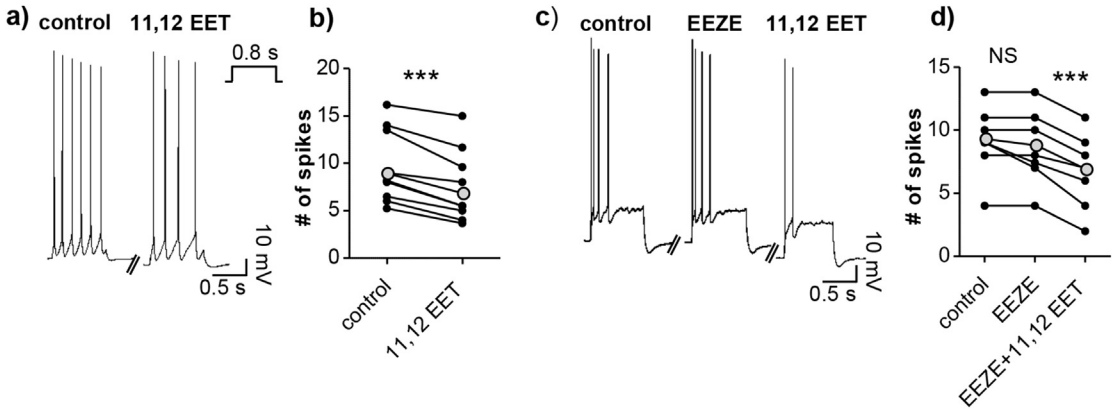

Fig. 5. 11,12 EET decreases excitability in CA1 PCs.
a) Representative current-clamp recording of a CA1 PC with response to somatic current injection (80 pA) before (left) and after the application of 11,12 EET (2 μM, right); b) Graph showing how the number of spikes in individual CA1 PCs (black circles) changes in presence of 11,12 EET (2 μM). The average of all cells is shown in gray circles; c) Representative current-clamp recording of a CA1 PC with response to somatic current injection (130 pA) before (left) and after the application of EEZE (10 μM, middle), followed by application of 11,12 EET (2 μM, right); d) Graph showing how the number of spikes in individual PCs (black circles) changes in presence of EEZE (10 μM) followed by 11,12 EET (2 μM). Average of all cells is shown in gray circles. $p < 0.001^{***}$.

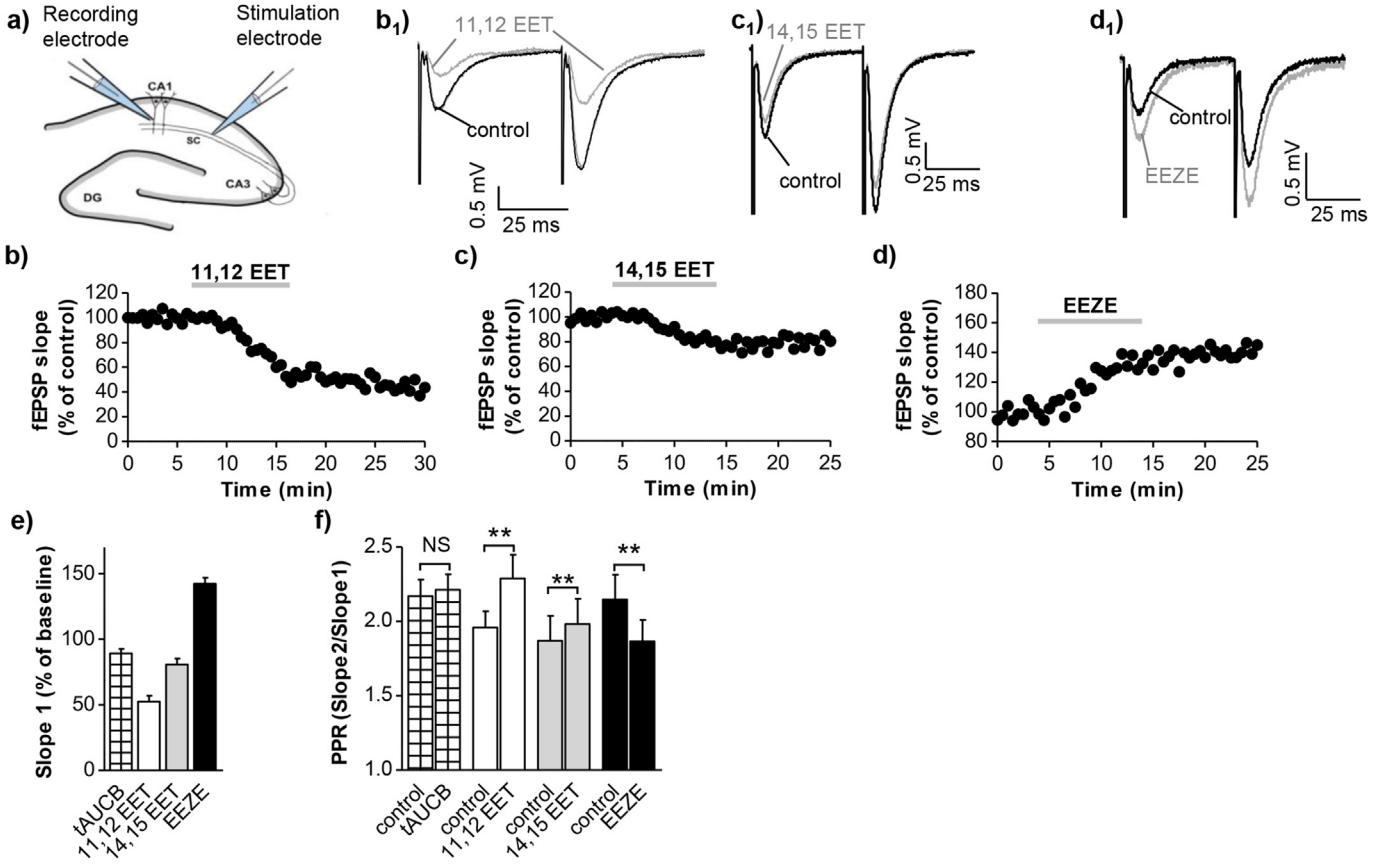

Fig. 6. 11,12 EET and 14,15 EET decrease, EEZE potentiates hippocampal fEPSPs.
a) Schematic drawing of a hippocampal slice, showing the localization of recording and stimulation electrode; b) Representative fEPSP slope vs. time graph with the application of 11,12 EET (2 μM) indicated by the gray horizontal line; b_1) Average of 20–30 traces before and after application of 11,12 EET; c) and c_1) Same as b) and b_1) for 14,15 EET (2 μM); d) and d_1) Same as b) and b_1) for EEZE (10 μM); e) Summary graph showing the effects of the different compounds on fEPSP slope 1; 1-way ANOVA followed by Bonferroni post hoc analysis: all comparisons $p < 0.001^{***}$ except for tAUCB vs 14,15 EET. For further statistics employing paired Student's *t* test see Table 1; f) Both EET regioisomers and EEZE change the respective PPRs significantly, pointing towards a presynaptic mechanism. DG dentate gyrus; SC Schaffer collaterals. $p < 0.01^{**}$.

end stimulating and recording electrodes were both placed in stratum radiatum on SCs (see scheme, Fig. 6a) and fEPSPs, evoked by two consecutive stimuli with an interstimulus interval of 50 ms, were recorded with inhibitory transmission left intact. Although under these conditions inhibition is not recorded directly, it is known to substantially modulate and shape hippocampal fEPSPs (Chapman et al., 1998). Unexpectedly, application of tAUCB (1 μM) resulted in a small, but significant decrease of fEPSP slopes and amplitudes, presumably due to effects exerted by accumulation of endogenous EETs (Fig. 6e, Table 1). Subsequent application of 11,12

Table 1
Summary of effects on fEPSPs.

Substance	Slope 1	Slope 2	Amp1	Amp2	*n*	Compared to
tAUCB (1 μM)	89.2 ± 3.2*	90.8 ± 3.0*	91.4 ± 3.2*	92.2 ± 3.1*	8	untreated
11,12 EET (2 μM)	52.4 ± 4.5***	60.2 ± 4.0***	52.8 ± 4.6***	59.4 ± 5.2**	7	tAUCB
14,15 EET (2 μM)	80.8 ± 4.6*	85.5 ± 4.2*	84.5 ± 5.0*	86.1 ± 4.3*	7	tAUCB
EEZE (10 μM)	142.2 ± 4.6***	123.3 ± 3.0**	136.1 ± 9.1**	125.5 ± 5.3**	7	untreated

Values are given as mean percentage ±SEM. For each compound normalized comparisons were carried out as indicated in the furthest column to the right. Asterisks indicate the significant difference obtained from these comparisons. ($p < 0.05^{*}$, $p < 0.01^{**}$, $p < 0.001^{***}$, paired Student's *t* test). *n* number of experiments performed.

EET led to a significant reduction of fEPSP slope1 to 52.4 ± 4.5% and slope2 to 60.2 ± 4.0%, respectively (Fig. 6b,b_1,e; for detailed data and fEPSP statistics, see Table 1). In comparison to 11,12 EET, 14,15 EET was less potent, only reducing fEPSP slope1 to 80.8 ± 4.6% of baseline values (see Fig. 6c, c_1, e). Both 11,12 EET and 14,15 EET significantly increased the PPR (Fig. 6f), further supporting the existence of a presynaptic target. By contrast, EEZE markedly potentiated fEPSP slope 1 and amplitude 1 to 140% and 136%, respectively (Fig. 6d, d_1, e). Since the potentiating effect was less pronounced for the second slope and amplitude, the PPR decreased under EEZE (Fig. 6f), again consistent with previous observations pointing towards a presynaptic site of action. Taken together, 11,12 and 14,15 EETs both reduce excitatory neurotransmission in the hippocampus with 11,12 EET being the more potent of the two. By contrast, EEZE increases excitatory transmission in the hippocampus, and is not capable of antagonizing the EET-mediated reduction.

3.5. tAUCB effect on epileptic discharges in the hippocampal formation

The tAUCB-mediated reduction of fEPSPs suggested that recordings from a population of neurons (rather than from a single neuron) might allow for the detection of effects exerted by endogenous EETs, released and accumulated in the brain slice. In a final experiment we therefore addressed the effect of tAUCB on epileptiform activity in brain slices. It is known that reduced GABAergic inhibition easily leads to large-scale synchronization and epileptic discharges in the hippocampal network. Thus, we applied bicuculline and, to get a better estimate of the synchronous action potential firing, recorded population spikes by placing the recording electrode on the stratum pyramidale. As expected, bicuculline (25 μM) led to a dramatic change in the waveform of single-pulse evoked population spikes (see Fig. 7a) and also substantially increased their amplitude and duration. To quantify the intensity of these epileptic-like bursts, we chose the so-called coastline bursting index CBI (Korn et al., 1987; Riekki et al., 2008). Essentially, beginning and end of the burst waveform were marked and the total duration was measured (see arrows in Fig. 7a). After 10 min, application of bicuculline resulted in a marked increase in CBI from 25.6 ± 1.5 to 62.0 ± 3.7 ms ($p = 0.00062^{***}$, $n = 5$, paired Student's *t* test). By contrast, tAUCB (1 μM) reduced the CBI slightly, but significantly (Fig. 7b, d; $p = 0.0077^{**}$, $n = 6$). When bicuculline was subsequently applied, it led to much less dramatic bursting (Fig. 7b,d) compared to bicuculline alone (Fig. 7e, unpaired Student's *t* test $p = 0.000136^{***}$). This showed that tAUCB, most likely via stabilizing endogenous EETs, is capable of reducing epileptiform discharges in brain slices consistent with recent data obtained in systemic epilepsy models in rodents.

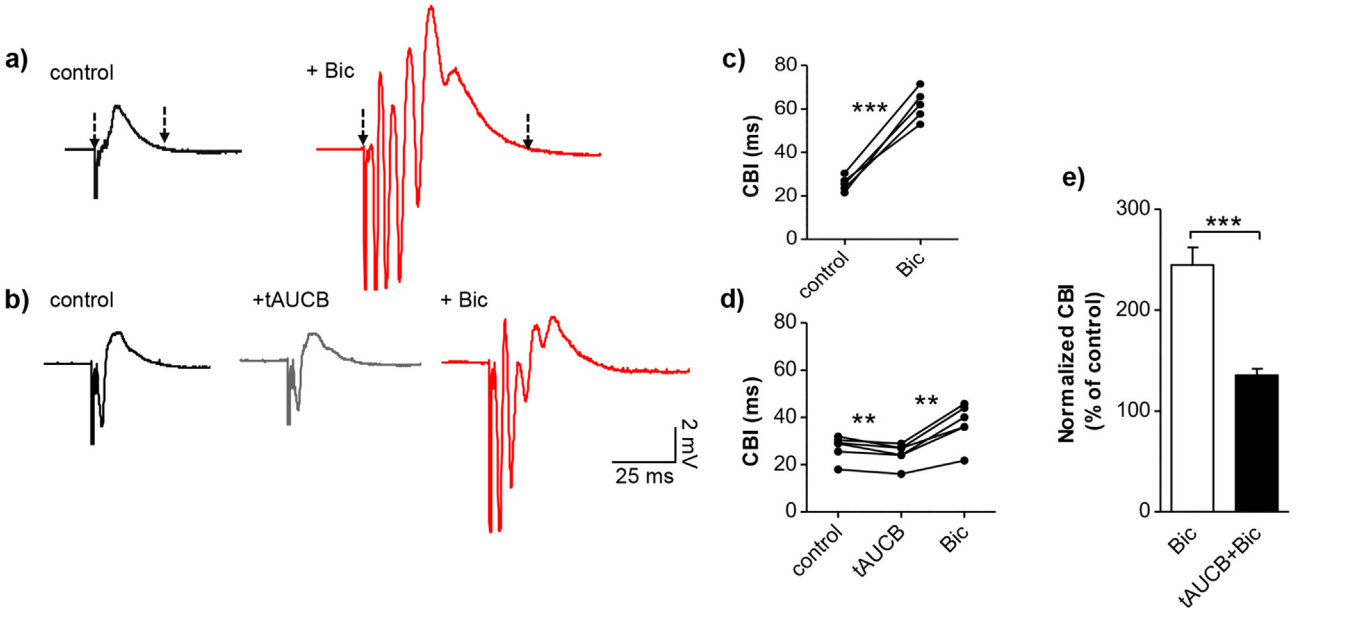

Fig. 7. tAUCB attenuates burst-like activity in the hippocampal formation.
a) Representative graphs of single-pulse evoked population spikes recorded from stratum pyramidale under control conditions (untreated slice; left) and 10 min after washing in of bicuculline (25 μM; right). Arrows indicate the total duration, used to calculate the respective CBI; b) Representative graphs of single-pulse evoked population spikes recorded under control conditions (untreated slice; left), after application of tAUCB (1 μM; middle), which was followed by application of bicuculline (25 μM; right). tAUCB and bicuculline graphs were taken each 10 min after start of bath-application of the respective compound; c) Summary graph for a), showing how CBI in individual experiments changes after application of bicuculline; d) Summary graph for b), showing how CBI changes under tAUCB and subsequently under bicuculline; e) Comparison of the normalized CBI observed under bicuculline on untreated slices and the CBI observed in slices pretreated with tAUCB. $p < 0.01^{**}$; $p < 0.001^{***}$.

4. Discussion

The present study has four major findings: First, 11,12 EET and to a lesser degree 14,15 EET inhibit EPSCs and fEPSPs in the hippocampus, thus reducing excitatory transmission. Second, 11,12 EET exerts its effect by acting on both pre- and postsynaptic targets in CA1 PCs, whereas the 14,15 EET-mediated effect seems limited to a presynaptic target. Third, postsynaptically, 11,12 EET opens a K^+ conductance via activation of a G protein, resulting in hyperpolarization and attenuated excitability of CA1 PCs. Finally, the functional antagonist EEZE seems to exclusively act via a presynaptic target, which with high probability differs from the one activated by 11,12 EET.

4.1. 11,12 EET-mediated hyperpolarization involves the opening of GIRK1/4 channels most likely via activation of $G_{\alpha i/o}$ proteins

We observed a 11,12 EET-specific opening of a hyperpolarizing current, which we identified as a K^+ current due to its reversal potential and the fact that it could be blocked by intracellular Cs^+. Since dialyzing the cell with the G protein blocker GDPβS prevented the EET-mediated opening of the K^+ current, a direct effect of EETs appeared unlikely and suggested that the activation of a G protein is a prerequisite. Both $BaCl_2$ and tertiapin Q blocked the 11,12 EET-mediated opening of the K^+ conductance and these findings together with the IV-curve (Fig. 4a) provide compelling evidence that 11,12 EET opens a GIRK channel in CA1 PCs. GIRKs usually require activation by the β/γ subunit of $G_{i/o}$ proteins, whereas G_s proteins only activate GIRK under nonphysiological conditions (e.g. following overexpression) (Dascal and Kahanovitch, 2015). However, studies focusing on intracellular pathways activated by EETs exclusively reported the involvement of G_s proteins. It needs to be noted, however, that all these studies used non-neuronal cells, e.g. endothelial cells (Ding et al., 2014; Node et al., 2001), preglomerular microvessels (Carroll et al., 2006), coronary arteries (Li and Campbell, 1997) and HEK cells (Fukao et al., 2001), implying that the cell type is of central importance as to which G protein is activated by EETs. Taken together, our discovery of the 11,12 EET-mediated opening of a GIRK channel, including the activation of $G_{i/o}$ proteins, constitutes a so far undescribed, new cellular pathway. This result may also shed new light on previous findings that EETs contribute to μ-opioid receptor-mediated anti-nociception (Conroy et al., 2010; Terashvili et al., 2008), a GPCR system commonly linked to $G_{i/o}$ proteins.

4.2. Potential postsynaptic targets for 11,12 EET in CA1 PCs

A large body of data, accumulated over the last three decades, suggests that EETs act through a specific binding site, most likely a cell surface receptor (Chen et al., 2009; Falck et al., 2003; Snyder et al., 2002). Because the majority of EET-mediated physiological responses occur with nanomolar concentrations, the existence of a high-affinity EET-receptor was proposed. We used low micromolecular concentrations (2 μM) of 11,12 EET throughout our study, but it is difficult to relate that to the final concentration reaching to the recording spot in brain slice. Tissue preparations are notorious for their ability to take up and sequester lipophilic, detergent-like compounds like EETs, which was also evident in our recordings as EET-mediated effects were difficult to reverse via wash out (see Fig. 6b with the effect lingering for 20 min after EET application). Furthermore, in our hands 11,12 EET concentrations in the nanomolar range produced extremely inconsistent results, often failing to elicit any response, which we attributed to the highly lipophilic nature of the compound. As a result, it was not possible to establish a meaningful dose-response relation and we decided to use a fixed concentration that gave reproducible results.

Although an EET-specific GPCR still awaits identification, some well-characterized GPCRs have been identified to which EETs, and specifically 11,12 EET, reportedly bind; these include the cannabinoid receptors CB1 and CB2, the dopamine receptor D3 and the GPR40. However, it takes 11,12 EET concentrations in the 100 micromolar range to displace high-affinity radio ligands from CB1, CB2 and D3 receptors (Inceoglu et al., 2007). EC_{50} values for the human GPR 40 are in a comparatively lower range with 6–8 μM (Itoh et al., 2003). Still, the GPR 40 constitutes an unlikely candidate for two reasons: 1.) EETs and DHETs were shown to activate the GPR40 to a similar degree (Itoh et al., 2003), while in our study only 11,12 EET, but not the corresponding DHET, was capable to activate a GIRK channel (see Fig. 4g). Furthermore, the GPR 40 is reportedly coupled to $G_{q/11}$ (Briscoe et al., 2003) and thus highly unlikely to activate a GIRK channel, which is classically linked to $G_{i/o}$ proteins (Dascal and Kahanovitch, 2015). Recently, 105 GPCRs were screened for their ability to respond to 14,15 EET, but unfortunately not 11,12 EET. While several GPCRs responded to micromolecular concentrations of 14,15 EET (the top five all being prostaglandin receptors), none could be identified meeting the criteria for a high-affinity receptor (Liu et al., 2016a). Similar unsatisfactory results with a smaller number of GPCRs, none of them responsive to 14,15 EET, were reported earlier in a study by Behm and colleagues (Behm et al., 2009), in which 14,15 EET was ultimately identified as an antagonist of native thromboxane receptors. Given our results, in which 11,12 EET shows distinct actions on GIRKs, it seems desirable to repeat these screenings with 11,12 EET.

4.3. Presynaptic effects mediated by 11,12 EET and possible molecular targets

Both EET regioisomers and EEZE modulate the PPR of evoked EPSCs and fEPSPS, which is consistent with a presynaptic mechanism. Notably, EEZE can a) not block the 11,12 EET-mediated reduction of EPSCs and b) changes mEPSC frequency, which 11,12 EET does not. These observations suggest distinct molecular mechanisms and targets for EEZE and EET. Specifically, the inability of 11,12 EET to alter mEPSC frequency strongly implies that its potential target requires action potential-induced depolarization. Possible candidates include therefore voltage-dependent ion channels such as Ca^{2+} or K^+ channels. The BK_{Ca} channel is an attractive candidate, given both the extensive data on its interaction with EETs and the fact that it is located on presynaptic sites in the CNS. However, at the CA3-CA1 synapse, from which we recorded, BK_{Ca} channels are not recruited under basal condition, but only under extreme conditions as in epileptic states and ischemia (Hu et al., 2001; Runden-Pran et al., 2002). The cardiac L-type Ca^{2+}channel may be another possible target. Interestingly, it is inhibited by nanomolar concentrations of 11,12 EET (Chen et al., 1999), but activated by higher concentrations of EETs via the cAMP/PKA system (Xiao et al., 1998, 2004). However, data showing CNS-residing Ca^{2+} channels interacting with EETs are still lacking. Finally, members of the TRPV family might be activated by EETs in the hippocampus. Particularly the TRPV1 channel family seems an eligible target, as it depresses glutamatergic synaptic transmission upon activation by another AA derivative, 12-(S)-HPETE (Gibson et al., 2008). While this effect seems similar to the one we observed with EETs, TRPV1 channels are exclusively located at excitatory synapses on hippocampal interneurons, excluding them as possible EETs targets on CA3-CA1 synapses. 11,12 EET was also reported to activate a TRPV4-TRPC1-BK_{Ca} complex in smooth muscle cells (Ma et al., 2015), but it remains to be proven if such channel complexes are also existent in neurons. More work is needed to identify the proper presynaptic targets for 11,12 and

14,15 EETs as well as EEZE.

4.4. EEZE effects on hippocampal neurotransmission

It is difficult to clearly conclude from our experiments, if the presynaptic effect exerted by EEZE is attributable to the antagonization of EET- mediated action or if EEZE elicits an effect by itself. Importantly, at least in two types of experiments EEZE was applied alone (mEPSC recordings, Fig. 2b; fEPSP recordings, Fig. 6d) on slices, which were not pretreated with tAUCB (tAUCB application was limited to experiments in which EETs were washed in). Thus, levels of ambient EETs were not elevated, making it less plausible that EEZE action reflects the blockade of an augmented endogenous EET tone.

On the postsynaptic site, EEZE unarguably failed to elicit any antagonistic actions; in fact, it showed no postsynaptic activity at all, since it neither modulated mEPSC kinetics and amplitudes, nor did it affect I_{hold} or RMP. The inability of EEZE to antagonize EET activity in neurons is not entirely unexpected; EEZE has shown inconsistent effects before with the most remarkably being that it vasodilates murine mesenteric arteries to a similar extent as a stable EET analogue (Harrington et al., 2004).

4.5. tAUCB and its effect on fEPSPs and epileptiform activity in brain slices

The sEHi tAUCB has been used in several recent studies to investigate the effect of endogenous EETs (e.g. Akhnokh et al., 2016; Imig et al., 2012). In our first experiments focusing on EPSCs in single cells, tAUCB alone did not show any effect; however in field recording, tAUCB significantly reduced fEPSP slopes and amplitudes. An explanation might be that the tAUCB effect is too small to be successfully measured in a single neuron, but becomes apparent when recordings from a whole population of neurons with synchronized activity are carried out. In fact, in the current study a similar phenomenon could be observed with bicuculline, as the $GABA_A$ receptor antagonist allowed for the undisturbed isolation of evoked EPSCs in single pyramidal cells, but led to epileptiform activity in field recording. Interestingly, the tAUCB effect on fEPSPs in absence of any $GABA_A$ receptor antagonists (Fig. 6), thus with intact inhibition, was small, since it generated on average only a 10% reduction. Such a slight effect might be due to comparatively low spontaneous activity and weak extracellular stimulation in the slice, which elicits only low Ca^{2+} influx into astrocytes and/or neurons and results in the release of respectively low quantities of EETs. Nevertheless, these amounts of endogenous EETs appeared to be sufficient to dampen subsequent bicuculline-induced epileptic bursts recorded from the somata of CA1 PCs (Fig. 7). However, tAUCB results should be interpreted with caution, as DHA or EPA-derived epoxides may also accumulate in the presence of tAUCB and are likely capable to interfere with neuronal transmission.

In summary, this study demonstrates for the first time that EETs have complex and regioisomer-specific pre- and postsynaptic actions in the hippocampus, including the 11,12 EET-mediated opening of a GIRK channel. These findings not only reveal a so far unknown signaling pathway of EETs, but may also help to explain their therapeutic potential in reducing epileptiform activity.

Funding

This work was supported by the Swiss National Foundation (grant PDFMP_127330, M.A.).

Acknowledgements

We thank Urs Gerber and George Hausmann for their helpful comments and careful reading of the manuscript.

Appendix A. Supplementary data

Supplementary data related to this article can be found at http://dx.doi.org/10.1016/j.neuropharm.2017.05.013.

References

Akhnokh, M.K., Yang, F.H., Samokhvalov, V., Jamieson, K.L., Cho, W.J., Wagg, C., Takawale, A., Wang, X., Lopaschuk, G.D., Hammock, B.D., Kassiri, Z., Seubert, J.M., 2016. Inhibition of soluble epoxide hydrolase limits mitochondrial damage and preserves function following ischemic injury. Front. Pharmacol. 7, 133.

Al-Anizy, M., Horley, N.J., Kuo, C.W., Gillett, L.C., Laughton, C.A., Kendall, D., Barrett, D.A., Parker, T., Bell, D.R., 2006. Cytochrome P450 Cyp4x1 is a major P450 protein in mouse brain. FEBS J. 273, 936–947.

Alkayed, N.J., Birks, E.K., Narayanan, J., Petrie, K.A., Kohler-Cabot, A.E., Harder, D.R., 1997. Role of P-450 arachidonic acid epoxygenase in the response of cerebral blood flow to glutamate in rats. Stroke 28, 1066–1072.

Behm, D.J., Ogbonna, A., Wu, C., Burns-Kurtis, C.L., Douglas, S.A., 2009. Epoxyeicosatrienoic acids function as selective, endogenous antagonists of native thromboxane receptors: identification of a novel mechanism of vasodilation. J. Pharmacol. Exp. Ther. 328, 231–239.

Briscoe, C.P., Tadayyon, M., Andrews, J.L., Benson, W.G., Chambers, J.K., Eilert, M.M., Ellis, C., Elshourbagy, N.A., Goetz, A.S., Minnick, D.T., Murdock, P.R., Sauls Jr., H.R., Shabon, U., Spinage, L.D., Strum, J.C., Szekeres, P.G., Tan, K.B., Way, J.M., Ignar, D.M., Wilson, S., Muir, A.I., 2003. The orphan G protein-coupled receptor GPR40 is activated by medium and long chain fatty acids. J. Biol. Chem. 278, 11303–11311.

Campbell, W.B., Gebremedhin, D., Pratt, P.F., Harder, D.R., 1996. Identification of epoxyeicosatrienoic acids as endothelium-derived hyperpolarizing factors. Circ. Res. 78, 415–423.

Capdevila, J.H., Falck, J.R., Harris, R.C., 2000. Cytochrome P450 and arachidonic acid bioactivation. Molecular and functional properties of the arachidonate monooxygenase. J. Lipid Res. 41, 163–181.

Carroll, M.A., Doumad, A.B., Li, J., Cheng, M.K., Falck, J.R., McGiff, J.C., 2006. Adenosine2A receptor vasodilation of rat preglomerular microvessels is mediated by EETs that activate the cAMP/PKA pathway. Am. J. Physiol. Ren. Physiol. 291, F155–F161.

Chapman, C.A., Perez, Y., Lacaille, J.C., 1998. Effects of GABA(A) inhibition on the expression of long-term potentiation in CA1 pyramidal cells are dependent on tetanization parameters. Hippocampus 8, 289–298.

Chen, J., Capdevila, J.H., Zeldin, D.C., Rosenberg, R.L., 1999. Inhibition of cardiac L-type calcium channels by epoxyeicosatrienoic acids. Mol. Pharmacol. 55, 288–295.

Chen, Y., Falck, J.R., Tuniki, V.R., Campbell, W.B., 2009. 20-125Iodo-14,15-epoxyeicosa-5(Z)-enoic acid: a high-affinity radioligand used to characterize the epoxyeicosatrienoic acid antagonist binding site. J. Pharmacol. Exp. Ther. 331, 1137–1145.

Conroy, J.L., Fang, C., Gu, J., Zeitlin, S.O., Yang, W., Yang, J., VanAlstine, M.A., Nalwalk, J.W., Albrecht, P.J., Mazurkiewicz, J.E., Snyder-Keller, A., Shan, Z., Zhang, S.Z., Wentland, M.P., Behr, M., Knapp, B.I., Bidlack, J.M., Zuiderveld, O.P., Leurs, R., Ding, X., Hough, L.B., 2010. Opioids activate brain analgesic circuits through cytochrome P450/epoxygenase signaling. Nat. Neurosci. 13, 284–286.

Dascal, N., Kahanovitch, U., 2015. The roles of gbetagamma and galpha in gating and regulation of GIRK channels. Int. Rev. Neurobiol. 123, 27–85.

Ding, Y., Fromel, T., Popp, R., Falck, J.R., Schunck, W.H., Fleming, I., 2014. The biological actions of 11,12-epoxyeicosatrienoic acid in endothelial cells are specific to the R/S-enantiomer and require the G(s) protein. J. Pharmacol. Exp. Ther. 350, 14–21.

Earley, S., Heppner, T.J., Nelson, M.T., Brayden, J.E., 2005. TRPV4 forms a novel Ca2+ signaling complex with ryanodine receptors and BKCa channels. Circ. Res. 97, 1270–1279.

Falck, J.R., Reddy, L.M., Reddy, Y.K., Bondlela, M., Krishna, U.M., Ji, Y., Sun, J., Liao, J.K., 2003. 11,12-epoxyeicosatrienoic acid (11,12-EET): structural determinants for inhibition of TNF-alpha-induced VCAM-1 expression. Bioorg. Med. Chem. Lett. 13, 4011–4014.

Fleming, I., Rueben, A., Popp, R., Fisslthaler, B., Schrodt, S., Sander, A., Haendeler, J., Falck, J.R., Morisseau, C., Hammock, B.D., Busse, R., 2007. Epoxyeicosatrienoic acids regulate Trp channel dependent Ca2+ signaling and hyperpolarization in endothelial cells. Arterioscler. Thromb. Vasc. Biol. 27, 2612–2618.

Fukao, M., Mason, H.S., Kenyon, J.L., Horowitz, B., Keef, K.D., 2001. Regulation of BK(Ca) channels expressed in human embryonic kidney 293 cells by epoxyeicosatrienoic acid. Mol. Pharmacol. 59, 16–23.

Gauthier, K.M., Deeter, C., Krishna, U.M., Reddy, Y.K., Bondlela, M., Falck, J.R., Campbell, W.B., 2002. 14,15-Epoxyeicosa-5(Z)-enoic acid: a selective epoxyeicosatrienoic acid antagonist that inhibits endothelium-dependent

hyperpolarization and relaxation in coronary arteries. Circ. Res. 90, 1028–1036.
Gibson, H.E., Edwards, J.G., Page, R.S., Van Hook, M.J., Kauer, J.A., 2008. TRPV1 channels mediate long-term depression at synapses on hippocampal interneurons. Neuron 57, 746–759.
Graves, J.P., Edin, M.L., Bradbury, J.A., Gruzdev, A., Cheng, J., Lih, F.B., Masinde, T.A., Qu, W., Clayton, N.P., Morrison, J.P., Tomer, K.B., Zeldin, D.C., 2013. Characterization of four new mouse cytochrome P450 enzymes of the CYP2J subfamily. Drug Metab. Dispos. 41, 763–773.
Harrington, L.S., Falck, J.R., Mitchell, J.A., 2004. Not so EEZE: the 'EDHF' antagonist 14, 15 epoxyeicosa-5(Z)-enoic acid has vasodilator properties in mesenteric arteries. Eur. J. Pharmacol. 506, 165–168.
Hayabuchi, Y., Nakaya, Y., Matsuoka, S., Kuroda, Y., 1998. Endothelium-derived hyperpolarizing factor activates Ca2+-activated K+ channels in porcine coronary artery smooth muscle cells. J. Cardiovasc Pharmacol. 32, 642–649.
Hu, H., Shao, L.R., Chavoshy, S., Gu, N., Trieb, M., Behrens, R., Laake, P., Pongs, O., Knaus, H.G., Ottersen, O.P., Storm, J.F., 2001. Presynaptic Ca2+-activated K+ channels in glutamatergic hippocampal terminals and their role in spike repolarization and regulation of transmitter release. J. Neurosci. 21, 9585–9597.
Hung, Y.W., Hung, S.W., Wu, Y.C., Wong, L.K., Lai, M.T., Shih, Y.H., Lee, T.S., Lin, Y.Y., 2015. Soluble epoxide hydrolase activity regulates inflammatory responses and seizure generation in two mouse models of temporal lobe epilepsy. Brain Behav. Immun. 43, 118–129.
Hwang, S.H., Tsai, H.J., Liu, J.Y., Morisseau, C., Hammock, B.D., 2007. Orally bioavailable potent soluble epoxide hydrolase inhibitors. J. Med. Chem. 50, 3825–3840.
Iliff, J.J., Fairbanks, S.L., Balkowiec, A., Alkayed, N.J., 2010a. Epoxyeicosatrienoic acids are endogenous regulators of vasoactive neuropeptide release from trigeminal ganglion neurons. J. Neurochem. 115, 1530–1542.
Iliff, J.J., Jia, J., Nelson, J., Goyagi, T., Klaus, J., Alkayed, N.J., 2010b. Epoxyeicosanoid signaling in CNS function and disease. Prostagl. Other Lipid Mediat 91, 68–84.
Imig, J.D., Simpkins, A.N., Renic, M., Harder, D.R., 2011. Cytochrome P450 eicosanoids and cerebral vascular function. Expert Rev. Mol. Med. 13, e7.
Imig, J.D., Walsh, K.A., Hye Khan, M.A., Nagasawa, T., Cherian-Shaw, M., Shaw, S.M., Hammock, B.D., 2012. Soluble epoxide hydrolase inhibition and peroxisome proliferator activated receptor gamma agonist improve vascular function and decrease renal injury in hypertensive obese rats. Exp. Biol. Med. (Maywood) 237, 1402–1412.
Inceoglu, B., Schmelzer, K.R., Morisseau, C., Jinks, S.L., Hammock, B.D., 2007. Soluble epoxide hydrolase inhibition reveals novel biological functions of epoxyeicosatrienoic acids (EETs). Prostagl. Other Lipid Mediat 82, 42–49.
Inceoglu, B., Zolkowska, D., Yoo, H.J., Wagner, K.M., Yang, J., Hackett, E., Hwang, S.H., Lee, K.S., Rogawski, M.A., Morisseau, C., Hammock, B.D., 2013. Epoxy fatty acids and inhibition of the soluble epoxide hydrolase selectively modulate GABA mediated neurotransmission to delay onset of seizures. PLoS One 8, e80922.
Itoh, Y., Kawamata, Y., Harada, M., Kobayashi, M., Fujii, R., Fukusumi, S., Ogi, K., Hosoya, M., Tanaka, Y., Uejima, H., Tanaka, H., Maruyama, M., Satoh, R., Okubo, S., Kizawa, H., Komatsu, H., Matsumura, F., Noguchi, Y., Shinohara, T., Hinuma, S., Fujisawa, Y., Fujino, M., 2003. Free fatty acids regulate insulin secretion from pancreatic beta cells through GPR40. Nature 422, 173–176.
Koerner, I.P., Jacks, R., DeBarber, A.E., Koop, D., Mao, P., Grant, D.F., Alkayed, N.J., 2007. Polymorphisms in the human soluble epoxide hydrolase gene EPHX2 linked to neuronal survival after ischemic injury. J. Neurosci. 27, 4642–4649.
Korn, S.J., Giacchino, J.L., Chamberlin, N.L., Dingledine, R., 1987. Epileptiform burst activity induced by potassium in the hippocampus and its regulation by GABA-mediated inhibition. J. Neurophysiol. 57, 325–340.
Lein, E.S., Hawrylycz, M.J., Ao, N., Ayres, M., Bensinger, A., Bernard, A., Boe, A.F., Boguski, M.S., Brockway, K.S., Byrnes, E.J., Chen, L., Chen, L., Chen, T.M., Chin, M.C., Chong, J., Crook, B.E., Czaplinska, A., Dang, C.N., Datta, S., Dee, N.R., Desaki, A.L., Desta, T., Diep, E., Dolbeare, T.A., Donelan, M.J., Dong, H.W., Dougherty, J.G., Duncan, B.J., Ebbert, A.J., Eichele, G., Estin, L.K., Faber, C., Facer, B.A., Fields, R., Fischer, S.R., Fliss, T.P., Frensley, C., Gates, S.N., Glattfelder, K.J., Halverson, K.R., Hart, M.R., Hohmann, J.G., Howell, M.P., Jeung, D.P., Johnson, R.A., Karr, P.T., Kawal, R., Kidney, J.M., Knapik, R.H., Kuan, C.L., Lake, J.H., Laramee, A.R., Larsen, K.D., Lau, C., Lemon, T.A., Liang, A.J., Liu, Y., Luong, L.T., Michaels, J., Morgan, J.J., Morgan, R.J., Mortrud, M.T., Mosqueda, N.F., Ng, L.L., Ng, R., Orta, G.J., Overly, C.C., Pak, T.H., Parry, S.E., Pathak, S.D., Pearson, O.C., Puchalski, R.B., Riley, Z.L., Rockett, H.R., Rowland, S.A., Royall, J.J., Ruiz, M.J., Sarno, N.R., Schaffnit, K., Shapovalova, N.V., Sivisay, T., Slaughterbeck, C.R., Smith, S.C., Smith, K.A., Smith, B.I., Sodt, A.J., Stewart, N.N., Stumpf, K.R., Sunkin, S.M., Sutram, M., Tam, A., Teemer, C.D., Thaller, C., Thompson, C.L., Varnam, L.R., Visel, A., Whitlock, R.M., Wohnoutka, P.E., Wolkey, C.K., Wong, V.Y., Wood, M., Yaylaoglu, M.B., Young, R.C., Youngstrom, B.L., Yuan, X.F., Zhang, B., Zwingman, T.A., Jones, A.R., 2007. Genome-wide atlas of gene expression in the adult mouse brain. Nature 445, 168–176.
Li, P.L., Campbell, W.B., 1997. Epoxyeicosatrienoic acids activate K+ channels in coronary smooth muscle through a guanine nucleotide binding protein. Circ. Res. 80, 877–884.
Li, R., Xu, X., Chen, C., Yu, X., Edin, M.L., Degraff, L.M., Lee, C.R., Zeldin, D.C., Wang, D.W., 2012. Cytochrome P450 2J2 is protective against global cerebral ischemia in transgenic mice. Prostagl. Other Lipid Mediat 99, 68–78.
Liu, X., Qian, Z.Y., Xie, F., Fan, W., Nelson, J.W., Xiao, X., Kaul, S., Barnes, A.P., Alkayed, N.J., 2016a. Functional screening for G protein-coupled receptor targets of 14,15-epoxyeicosatrienoic acid. Prostagl. Other Lipid Mediat. http://dx.doi.org/10.1016/j.prostaglandins.2016.09.002 (In press).
Liu, Y., Wan, Y., Fang, Y., Yao, E., Xu, S., Ning, Q., Zhang, G., Wang, W., Huang, X., Xie, M., 2016b. Epoxyeicosanoid signaling provides multi-target protective effects on neurovascular unit in rats after focal ischemia. J. Mol. Neurosci. 58, 254–265.
Lu, T., VanRollins, M., Lee, H.C., 2002. Stereospecific activation of cardiac ATP-sensitive K(+) channels by epoxyeicosatrienoic acids: a structural determinant study. Mol. Pharmacol. 62, 1076–1083.
Luo, G., Zeldin, D.C., Blaisdell, J.A., Hodgson, E., Goldstein, J.A., 1998. Cloning and expression of murine CYP2Cs and their ability to metabolize arachidonic acid. Arch. Biochem. Biophys. 357, 45–57.
Ma, Y., Zhang, P., Li, J., Lu, J., Ge, J., Zhao, Z., Ma, X., Wan, S., Yao, X., Shen, B., 2015. Epoxyeicosatrienoic acids act through TRPV4-TRPC1-KCa1.1 complex to induce smooth muscle membrane hyperpolarization and relaxation in human internal mammary arteries. Biochim. Biophys. Acta 1852, 552–559.
Marowsky, A., Burgener, J., Falck, J.R., Fritschy, J.M., Arand, M., 2009. Distribution of soluble and microsomal epoxide hydrolase in the mouse brain and its contribution to cerebral epoxyeicosatrienoic acid metabolism. Neuroscience 163, 646–661.
Morisseau, C., Inceoglu, B., Schmelzer, K., Tsai, H.J., Jinks, S.L., Hegedus, C.M., Hammock, B.D., 2010. Naturally occurring monoepoxides of eicosapentaenoic acid and docosahexaenoic acid are bioactive antihyperalgesic lipids. J. Lipid Res. 51, 3481–3490.
Node, K., Ruan, X.L., Dai, J., Yang, S.X., Graham, L., Zeldin, D.C., Liao, J.K., 2001. Activation of Galpha s mediates induction of tissue-type plasminogen activator gene transcription by epoxyeicosatrienoic acids. J. Biol. Chem. 276, 15983–15989.
Qu, W., Bradbury, J.A., Tsao, C.C., Maronpot, R., Harry, G.J., Parker, C.E., Davis, L.S., Breyer, M.D., Waalkes, M.P., Falck, J.R., Chen, J., Rosenberg, R.L., Zeldin, D.C., 2001. Cytochrome P450 CYP2J9, a new mouse arachidonic acid omega-1 hydroxylase predominantly expressed in brain. J. Biol. Chem. 276, 25467–25479.
Riekki, R., Pavlov, I., Tornberg, J., Lauri, S.E., Airaksinen, M.S., Taira, T., 2008. Altered synaptic dynamics and hippocampal excitability but normal long-term plasticity in mice lacking hyperpolarizing GABA A receptor-mediated inhibition in CA1 pyramidal neurons. J. Neurophysiol. 99, 3075–3089.
Runden-Pran, E., Haug, F.M., Storm, J.F., Ottersen, O.P., 2002. BK channel activity determines the extent of cell degeneration after oxygen and glucose deprivation: a study in organotypical hippocampal slice cultures. Neuroscience 112, 277–288.
Sanchez-Mejia, R.O., Newman, J.W., Toh, S., Yu, G.Q., Zhou, Y., Halabisky, B., Cisse, M., Scearce-Levie, K., Cheng, I.H., Gan, L., Palop, J.J., Bonventre, J.V., Mucke, L., 2008. Phospholipase A2 reduction ameliorates cognitive deficits in a mouse model of Alzheimer's disease. Nat. Neurosci. 11, 1311–1318.
Shen, H.C., 2010. Soluble epoxide hydrolase inhibitors: a patent review. Expert Opin. Ther. Pat. 20, 941–956.
Sisignano, M., Park, C.K., Angioni, C., Zhang, D.D., von Hehn, C., Cobos, E.J., Ghasemlou, N., Xu, Z.Z., Kumaran, V., Lu, R., Grant, A., Fischer, M.J., Schmidtko, A., Reeh, P., Ji, R.R., Woolf, C.J., Geisslinger, G., Scholich, K., Brenneis, C., 2012. 5,6-EET is released upon neuronal activity and induces mechanical pain hypersensitivity via TRPA1 on central afferent terminals. J. Neurosci. 32, 6364–6372.
Snyder, G.D., Krishna, U.M., Falck, J.R., Spector, A.A., 2002. Evidence for a membrane site of action for 14,15-EET on expression of aromatase in vascular smooth muscle. Am. J. Physiol. Heart Circ. Physiol. 283, H1936–H1942.
Sodickson, D.L., Bean, B.P., 1996. GABAB receptor-activated inwardly rectifying potassium current in dissociated hippocampal CA3 neurons. J. Neurosci. 16, 6374–6385.
Spector, A.A., Norris, A.W., 2007. Action of epoxyeicosatrienoic acids on cellular function. Am. J. Physiol. Cell Physiol. 292, C996–C1012.
Terashvili, M., Tseng, L.F., Wu, H.E., Narayanan, J., Hart, L.M., Falck, J.R., Pratt, P.F., Harder, D.R., 2008. Antinociception produced by 14,15-epoxyeicosatrienoic acid is mediated by the activation of beta-endorphin and met-enkephalin in the rat ventrolateral periaqueductal gray. J. Pharmacol. Exp. Ther. 326, 614–622.
Thompson, C.M., Capdevila, J.H., Strobel, H.W., 2000. Recombinant cytochrome P450 2D18 metabolism of dopamine and arachidonic acid. J. Pharmacol. Exp. Ther. 294, 1120–1130.
Vito, S.T., Austin, A.T., Banks, C.N., Inceoglu, B., Bruun, D.A., Zolkowska, D., Tancredi, D.J., Rogawski, M.A., Hammock, B.D., Lein, P.J., 2014. Post-exposure administration of diazepam combined with soluble epoxide hydrolase inhibition stops seizures and modulates neuroinflammation in a murine model of acute TETS intoxication. Toxicol. Appl. Pharmacol. 281, 185–194.
Vriens, J., Owsianik, G., Fisslthaler, B., Suzuki, M., Janssens, A., Voets, T., Morisseau, C., Hammock, B.D., Fleming, I., Busse, R., Nilius, B., 2005. Modulation of the Ca2 permeable cation channel TRPV4 by cytochrome P450 epoxygenases in vascular endothelium. Circ. Res. 97, 908–915.
Wang, Z., Wei, Y., Falck, J.R., Atcha, K.R., Wang, W.H., 2008. Arachidonic acid inhibits basolateral K channels in the cortical collecting duct via cytochrome P-450 epoxygenase-dependent metabolic pathways. Am. J. Physiol. Ren. Physiol. 294, F1441–F1447.
Watanabe, H., Vriens, J., Prenen, J., Droogmans, G., Voets, T., Nilius, B., 2003. Anandamide and arachidonic acid use epoxyeicosatrienoic acids to activate TRPV4 channels. Nature 424, 434–438.
Wu, H.F., Yen, H.J., Huang, C.C., Lee, Y.C., Wu, S.Z., Lee, T.S., Lin, H.C., 2015. Soluble epoxide hydrolase inhibitor enhances synaptic neurotransmission and plasticity in mouse prefrontal cortex. J. Biomed. Sci. 22, 94.
Xiao, Y.F., Huang, L., Morgan, J.P., 1998. Cytochrome P450: a novel system

modulating Ca2+ channels and contraction in mammalian heart cells. J. Physiol. 508 (Pt 3), 777–792.
Xiao, Y.F., Ke, Q., Seubert, J.M., Bradbury, J.A., Graves, J., Degraff, L.M., Falck, J.R., Krausz, K., Gelboin, H.V., Morgan, J.P., Zeldin, D.C., 2004. Enhancement of cardiac L-type Ca2+ currents in transgenic mice with cardiac-specific overexpression of CYP2J2. Mol. Pharmacol. 66, 1607–1616.
Zhang, W., Koerner, I.P., Noppens, R., Grafe, M., Tsai, H.J., Morisseau, C., Luria, A., Hammock, B.D., Falck, J.R., Alkayed, N.J., 2007. Soluble epoxide hydrolase: a novel therapeutic target in stroke. J. Cereb. Blood Flow. Metab. 27, 1931–1940.
Zou, A.P., Fleming, J.T., Falck, J.R., Jacobs, E.R., Gebremedhin, D., Harder, D.R., Roman, R.J., 1996. Stereospecific effects of epoxyeicosatrienoic acids on renal vascular tone and K(+)-channel activity. Am. J. Physiol. 270, F822–F832.

Abbreviations

AA: arachidonic acid
ACSF: artificial cerebrospinal fluid
AUDA: 12-(3-adamantan-1-yl-ureido) dodecanoic acid
BK_{Ca}: calcium-acitivated big potassium
CA: cornu ammonis
CYP: cytochrome P450-dependent monooxygenase
DHA: docosahexaenoic acid
DHET(s): dihydroxyeicosatrienoic acid(s)
EET(s): epoxyeicosatrienoic acid(s)
EEZE: 14,15 epoxyeicosa-5(Z)-enoic acid
EPSC: excitatory postsynaptic current
EPA: eicosapentaenoic acid
fEPSP: field excitatory postsynaptic potential
GABA: γ-aminobutyric acid
GDPβS: guanosine-5′-O-2-thiodiphosphate
GIRK: G protein coupled/gated inward rectifying potassium
12-HPETE: 12-hydroperoxyeicosatetraenoic acid
I_{hold}: holding current
mEPSC(s): miniature excitatory postsynaptic current(s)
PPR: paired pulse ratio
PC(s): pyramidal cell(s)
RMP: resting membrane potential
SC(s): Schaffer collateral(s)
sEH: soluble epoxide hydrolase
sEHi: soluble epoxide hydrolase inhibitor
tAUCB: trans-4-[4-(3-adamantan-1-y1-ureido)-cyclohexyloxy]-benzoic acid
TTQ: tertiapin Q
TTX: tetrodotoxin